Algorithm Theoretical Basis Document

Semi-Analytical CloUd Retrieval Algorithm for

SCIAMACHY/ENVISAT

Alexander A. Kokhanovsky, Vladimir V. Rozanov,
Marco Vountas, Wolfhardt Lotz, Heinrich Bovensmann, John P. Burrows

Institute of Environmental Physics, University of Bremen, Otto Hahn Allee 1
D-28334 Bremen, Germany

Phone: 49-421-218-2915
Fax: 49-421-218-4555
alexk@iup.physik.uni-bremen.de

April 1st, 2006

Contents

1. Introduction

Clouds play an important role in the Earth climate system (Kondratyev and Binenko, 1984; Liou, 1992). The amount of radiation reflected by the Earth-atmosphere system into outer space depends not only on the cloud cover and the total amount of condensed water in the Earth atmosphere but also the size of droplets a_{ef} and their thermodynamic state is also of importance.

The information about microphysical properties and spatial distributions of terrestrial clouds on a global scale can be obtained only with satellite remote sensing systems. Different spectrometers and radiometers (Bovensmann et al.,1999; Deschamps et al., 1994; King et al., 1992; Nakajima et al., 1998), deployed on space-based platforms, measure the angular and spectral distribution of intensity and polarization of reflected solar light. Generally, the measured values depend both on geometrical and microphysical characteristics of clouds. Thus, the inherent properties of clouds can be retrieved (at least in principle) by the solution of the inverse problem. The accuracy of the retrieved values depends on the accuracy of measurements and the accuracy of the forward radiative transfer model.

In particular, it is often assumed that clouds can be represented by homogeneous plane-parallel slabs infinitely extended in the horizontal direction (Goloub et al., 2000; Han et al., 1994; King, 1981, 1987; Nakajima and King, 1990, 1991; Rossow, 1989; Rossow and Schiffer, 1999; Kokhanovsky et al., 2003). The range of applicability of such an assumption for real clouds is very limited as is shown by observations of light from the sky on a cloudy day. For example, the retrieved cloud optical thickness τ is apparently dependent on the viewing geometry (Loeb and Davies, 1996, Loeb and Coakley, 1998). This, of course, would not be the case for an idealized plane-parallel cloud layer. However, both the state-of-art radiative transfer theory and computer technology are not capable to incorporate 3-D effects into operational satellite retrieval schemes. As a result, cloud parameters retrieved should be considered as a rather coarse approximation to reality.

However, even such limited tools produce valuable information on terrestrial clouds properties. For example, it was confirmed by satellite measurements that droplets in clouds over oceans are usually larger than those over land (Han et al., 1994). This feature, for instance, is of importance for the simulation of the Earth's climate (Slingo, 1989).

A new Semi-Analytical CloUd Retrieval Algorithm (SACURA) for the cloud liquid water path and water droplets size determination presented here is based on the asymptotical solution of the radiative transfer equation for a special case of disperse media, having a large optical thickness. This solution was obtained by Germogenova (1961, 1963) for plane-parallel turbid slabs. Such an approach has already been used in a number of studies (Rozenberg, 1978; King, 1987). The difference with our technique is that the asymptotical solutions are further simplified such that the inverse problem is reduced to the solution of a single transcendent equation. This allows us to speed up the retrieval process significantly without the substantial loss of the accuracy of the retrieved parameters.

The algorithm is restricted to the case of optically thick clouds (the optical thickness $\tau \geq 5$). It is planned to be supplemented in the future by the exact radiative transfer

calculations at $\tau < 5$ (Nakajima and King, 1990). However, it should be stressed that the optical thickness is highly correlated with the geometrical thickness of clouds. For instance, it was shown (Feigelson, 1981) that clouds with $\tau < 5$ have the geometrical thickness less than 200*m* on average. It is difficult to expect that such clouds are homogeneous in the horizontal direction. This leads to the horizontal photon transport (Cahalan et al., 1994; Platnick, 2001), which is not considered in standard retrieval procedures (Arking and Childs, 1985; Nakajima and King, 1990; Platnick et al., 2001). Therefore, the LUT approach for thin clouds is much less accurate as compared to the case of thick clouds.

Apart a_{ef} and τ, we also retrieve the liquid water path $w\left(gm^{-2}\right)$. The cloud albedo r and the columnar concentration of droplets $N(m^{-2})$ can be easily obtained from a_{ef}, w using well-known relationships between these quantities (see below).

The cloud top height is derived from measurements in the oxygen A-absorption band as recommended by Yamamoto and Wark (1961). Such an approach has been used extensively by many authors (Kuze and Chance, 1994; Fischer et al., 2000; Koelemeijer et al., 2001, 2002; Kuji and Nakajima, 2002; Kokhanovsky et al., 2006). This part of the retrieval is called SACURA-B as compared to SACURA-A aimed to retrievals of the pair $\left(a_{ef}, w\right)$. At the moment two parts of the retrieval scheme are decoupled.

Finally, the cloud thermodynamic state is obtained using different spectral signatures of liquid water as compared to ice in the spectral range 1550-1670nm (Pilewskie and Twomey, 1987a,b; Knap et al., 2002; Acaretta et al., 2004).

2. Forward model

2.1. Reflection function

The reflection function of a cloud $R\left(\vartheta_0, \vartheta, \varphi\right)$ is defined as the ratio of reflected light intensity $I^{\uparrow}\left(\vartheta_0, \vartheta, \varphi\right)$ for the case of a cloud to that of an ideal Lambertian white reflector:

$$R\left(\vartheta_0, \vartheta, \varphi\right) = \frac{I^{\uparrow}\left(\vartheta_0, \vartheta, \varphi\right)}{I^{*}\left(\vartheta_0\right)}, \tag{1}$$

where

$$I^{*}\left(\vartheta_0\right) = F \cos\vartheta_0 \tag{2}$$

is the intensity of light reflected from the ideally white Lambertian reflector, πF is the solar flux on the area perpendicular to the direction of incidence, ϑ_0 is the solar angle, ϑ is the observation angle and φ is the relative azimuth between solar and observation directions. It follows for the Lambertian ideally white reflector from Eq. (1): $R \equiv 1$. This result does not depend on the viewing geometry by definition. Although clouds are white when looking from space, their reflection function $R\left(\vartheta_0, \vartheta, \varphi\right)$ is not equal to one. It depends on the viewing geometry.

The results of calculations of the reflection function of an idealized semi – infinite nonabsorbing water cloud $R_\infty^0(\vartheta_0,\vartheta,\varphi)$ at the wavelength $\lambda = 650\ nm$ and the nadir observation are presented in Fig.1. Calculations were performed using the code developed by Mishchenko et al. (1999) for the gamma particle size distribution of water droplets (Deirmendjian, 1969):

$$f(a) = Aa^s e^{-s\frac{a}{a_0}} \quad , \tag{3}$$

where

$$A = \Gamma^{-1}(s+1)\left(\frac{s}{a_0}\right)^{s+1} \tag{4}$$

is the normalization constant and a_0 is the mode radius. The half-width parameter *s* was equal to 6. This value is typical for terrestrial clouds (Kokhanovsky, 2006). The effective radius, which is frequently used in cloud remote sensing studies, is defined as the ratio of the third to the second moment of the particle size distribution. In particular, it follows for the distribution , given by Eq. (3):

$$a_{ef} = a_0\left(1+\frac{3}{s}\right) \quad . \tag{5}$$

The values of a_{ef} were 6 and 16 micrometers in calculations given in Fig.1.

The values of R_∞^0 are larger than 1.0 for solar zenith angles smaller than 45° (see Fig.1). This implies that for such illumination conditions a semi-infinite cloud is even more reflective than the ideally white Lambertian surface. It follows from Fig.1 that the reflection function $R_\infty^0(\vartheta_0,\vartheta,\varphi)$ only weakly depends on the size of particles. So we neglect such a dependence in the cloud retrieval procedure. Then a water cloud with the Cloud C1 droplet size distribution is assumed (see Eq. (3) at *s=6*, $a_0 = 4\mu m$) and the phase function is calculated at the wavelength 443nm.

The reflectance over a partially cloudy field with the cloud fraction *c* is presented as

$$R=cR_c+(1-c)R_a, \tag{6}$$

where R_a is the reflection function of the background continental atmosphere defined in the framework of SCIATRAN and R_c is the cloud reflection function. Therefore, we derive:

$$R_c=c^{-1}R-c^{-1}(1-c)R_a. \tag{7}$$

Eq. (7) enables the reduction of a partially cloudy case to the case of completely cloud covered scene. This procedure is used by SACURA to treat partially cloudy scenes.

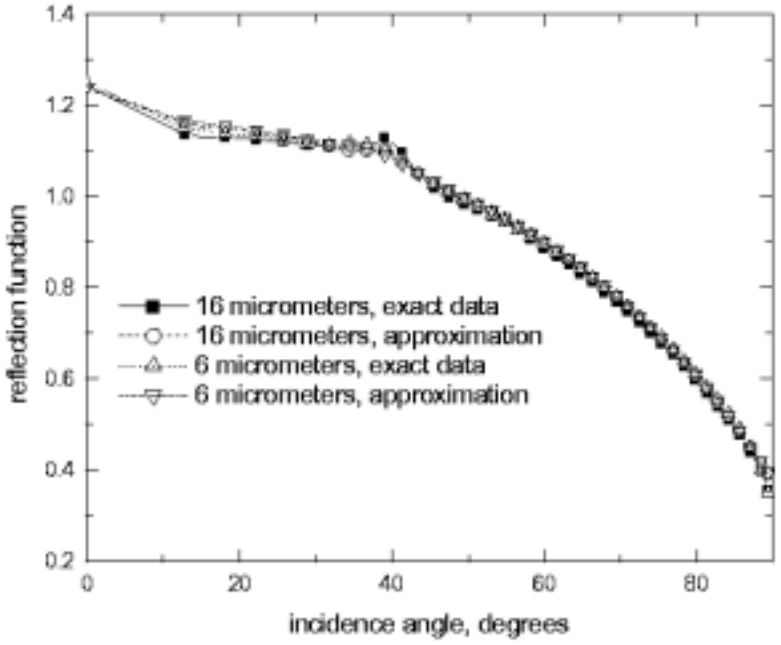

Fig. 1. The dependence of the reflection functions of semi-infinite clouds with effective radii $a_{ef} = 6,\ 16 \mu m$ at the nadir observation (see details in the text) on the solar zenith angle (Kokhanovsky, 2006). Exact results correspond to the data obtained using the radiative transfer code described by Mishchenko et al. (1999). The approximate results were obtained in the way as described by Kokhanovsky et al. (2003).

2.2. Asymptotic theory

The asymptotic solutions of the radiative transfer equation valid for optically thick media were derived by Germogenova (1961). They can be used for arbitrary local scattering laws and levels of absorption in the medium. The only limitation is that the optical thickness τ must be a large number. King (1987) found that the asymptotic theory is accurate to within 1% for $\tau \geq \tau^*$, where $\tau^* = 1.45\sigma$ with $\sigma = (1-g)^{-1}$. Here g is the asymmetry parameter of the local single scattering law. It means that $\tau^* = 145$ for biological media having *g=0.99.* Fortunately, the value of g is close to 0.85 for most of water clouds in the visible (Kokhanovsky, 2004a). This means that $\tau^* = 10$ and asymptotic theory is applicable to most of cases of extended cloudiness. The situation is even better for crystalline clouds. Then the value of g is close to 0.75 and $\tau^* = 6.0$.

The asymptotic solution for the cloud reflection function can be written in the following simple form (Germogenova, 1961, 1963; van de Hulst, 1980; Sobolev, 1984; Nakajima and King, 1992):

$$R(\mu,\mu_0,\varphi,\tau)=R_\infty(\mu,\mu_0,\varphi)-\frac{mle^{-2k\tau}}{1-l^2e^{-2k\tau}}K(\mu)K(\mu_0). \quad (8)$$

Here $R(\mu,\mu_0,\varphi,\tau)$ is the reflection function for a plane-parallel cloud layer. The values μ and μ_0 are cosines of the observation ϑ and incidence ϑ_0 angles, respectively, and φ is the relative azimuth. The function $R(\mu,\mu_0,\varphi,\tau)$ is defined as the ratio of the intensity I_r of reflected light for a turbid layer illuminated in the direction specified by the incidence angle ϑ_0 to the value of I_r for the absolutely white Lambertian screen as discussed above. There is a major problem associated with Eq. (8). It requires quite complex calculations of escape functions $K(\mu)$, reflection functions for a semi-infinite layer $R_\infty(\mu,\mu_0,\varphi)$ and parameters *k, l, m* using integral equations (Minin, 1988). Also matrix equations can be used for this purpose(Nakajima and King , 1992). The problem is simpler in the visible, where the absorption of light by clouds is negligible in most of cases and Eq. (8) transforms to the following result (van de Hulst, 1980):

$$R(\mu,\mu_0,\varphi,\tau)=R_\infty^0(\mu,\mu_0,\varphi)-t(\tau)K_0(\mu)K_0(\mu_0). \quad (9)$$

Here the "0"subscript means that the correspondent characteristic is calculated for the case of zero light absorption in the medium under study and

$$t(\tau)=\frac{1}{\alpha+0.75\tau(1-g)} \quad (10)$$

is the diffused transmittance of a cloud under the diffuse illumination. The parameter $\alpha\approx1.072$ does not vary considerably for media having different microstructures (King, 1987). Also it follows within the accuracy 2% (Kokhanovsky, 2004b):

$$K_0(\mu)=\frac{3}{7}[1+2\mu] \quad (11)$$

at $\mu\geq0.2$. Effectively, Eqs. (9)-(11) reduce the problem of the calculation of the reflection function of a finite cloud to that of a semi-infinite cloud (see Fig.1). This is of a great importance because the function $R_\infty^0(\mu,\mu_0,\varphi)$ depends only on the phase function and this dependence is rather weak (Kokhanovsky, 2004a). Therefore, correspondent LUTs in the cloud retrieval algorithms can be substantially reduced. Also one can use parameterisations of the function $R_\infty^0(\mu,\mu_0,\varphi)$, which enhances the speed of retrieval even further (Kokhanovsky et al., 2003). In particular, the following parameterization of this function can be used(Kokhanovsky, 2006):

$$R_\infty^0(\mu,\mu_0,\varphi)=\frac{A+B(\mu+\mu_0)+C\mu\mu_0+F(\theta)}{4(\mu+\mu_0)}. \quad (12)$$

The parameters *A, B, C* and the function $F(\theta)$ differ for different particulate media and can be found comparing calculations using Eq. (12) with numerical solutions of the radiative transfer equation (e.g., various least square minimization techniques can be used for this purpose). Note that $\theta=acos(-\mu\mu_0+ss_0\cos\varphi)$ is the scattering angle ($s=\sin\vartheta$, $s_0=\sin\vartheta_0$). Kokhanovsky (2004b) has shown that it follows for water clouds: *A=3.944, B=-2.5,*

C=10.664, and $F(\theta) = p(\theta) - \bar{p}(\theta)$, where $p(\theta)$ is the phase function. The bar means averaging with respect to the azimuth. It follows fro crystalline clouds (Kokhanovsky, 2006): *A=1.247, B=1.186, C=5.157,* and $F(\theta) \equiv p(\theta)$. Note that for most of applications one can neglect the small contribution due the last term in the nominator of Eq. (12).

It is of importance to have a simple formulation similar to that shown above for water clouds in the near –infrared (e.g., till the wavelength $2.25\,\mu m$, where many modern spectrometers and radiometers onboard various satellite platforms operate). This could be done either using parameterizations of functions and parameters given in Eq. (8) against the single scattering albedo ω_0 (Harshvardhan and King, 1986) or applying so-called exponential approximation (Zege et al., 1991). The next section is devoted to the derivation of the analytical expression for the reflection function of cloud fields in the modified exponential approximation.

2.3 Exponential approximation

The idea of the exponential approximation is quite simple. The main parameters and functions in Eq. (8) have following analytical forms for the small probability of photon absorption (PPA) $\beta = 1 - \omega_0$ (van de Hulst, 1980):

$$R_\infty(\mu,\mu_0,\varphi) = R_\infty^0(\mu,\mu_0,\varphi) \; - \; 4 \; \sqrt{\frac{\beta}{3(1\text{-g})}} K_0(\mu) K_0(\mu_0), \qquad (13)$$

$$K(\mu) = K_0(\mu)\left(1 - 2\alpha \; \sqrt{\frac{\beta}{3(1\text{-g})}}\right), \qquad (14)$$

$$k = \sqrt{3(1-g)\beta}\,, \quad l = 1 - 4\alpha\sqrt{\frac{\beta}{3(1\text{-g})}}\,, \qquad m = 8\sqrt{\frac{\beta}{3(1\text{-g})}}\,. \qquad (15)$$

These approximations are valid only for values of $\beta = \sigma_{abs} / \sigma_{ext} \le 0.0001$. Here σ_{abs} and σ_{ext} are absorption and extinction coefficients, respectively. For water clouds in the near-infrared β can reach *0.1* and even larger values (Kokhanovsky, 2004a). So we need to consider next terms in the expansions (13)-(15) (Minin, 1988). However, correspondent expressions appear to be extremely complicated for most of practical applications. Therefore, Zege et al. (1991) proposed following exponential forms for the reflection function $R_\infty(\mu,\mu_0,\varphi)$ and the combination $f(\mu,\mu_0) = mK(\mu)K(\mu_0)$ in Eq. (8):

$$R_\infty(\mu,\mu_0,\varphi) = R_\infty^0 \exp\left(-yu(\mu,\mu_0,\varphi)\right), \qquad (16)$$

$$f(\mu,\mu_0) = \left(1 - \exp(-2y)\right) K_0(\mu) K_0(\mu_0), \qquad (17)$$

where

$$y = 4\sqrt{\frac{\beta}{3(1-g)}}\,, \qquad u(\mu,\mu_0,\varphi) = \frac{K_0(\mu)K_0(\mu_0)}{R_\infty^0(\mu,\mu_0,\varphi)}\,. \qquad (18)$$

Similar exponential expression can be used for the parameter *l*. Namely, we have:

$$l = exp(-\alpha y). \qquad (19)$$

It should be stressed that these expressions transform in the exact asymptotic results given by Eqs. (13)-(15) as $\beta \to 0$. However, they allow us to extend the applicability of Eqs. (13)-(15) to larger values of β. Note that empirical exponential forms were appeared here not by chance but have deep roots related to the diffusion theory (Kokhanovsky, 2006). The substitution of Eqs. (10), (16)-(19) into Eq. (8) gives:

$$R(\mu,\mu_0,\varphi,\tau) = R_\infty^0 \exp\left(-yu(\mu,\mu_0,\varphi)\right) - te^{-x-y} K_0(\mu) K_0(\mu_0), \quad (20)$$

where we introduced a new parameter $x = k\tau$. The global transmittance t is given by:

$$t = \frac{\sinh y}{\sinh(\alpha y + x)}. \quad (21)$$

Eq. (20) transforms into Eq. (2) (and also Eq. (21) transforms into Eq. (10)) at $\beta = 0$. However, Eq. (20) unlike Eq. (9) allows to consider absorbing media as well. It is important that no new angular functions appear in Eq. (20) as compared to Eq. (9). This is in contrast with Eq. (8), where parameters and functions have an implicit and complex dependence on β. Eq. (20) can be used for the rapid estimations of light reflection from cloudy media and also for the speeding up cloud retrieval algorithms (Kokhanovsky et al., 2003). The range of applicability of the exponential approximation (20) can be extended using correction terms derived from the numerical solution of the radiative transfer equation. In particular, we find that the accuracy of Eq. (20) for cloudy media can be increased using following substitutions: $u \to u(1-0.05y)$, $t \to t - \Delta$, where

$$\Delta = \frac{a + b\mu\mu_0 + c\mu^2\mu_0^2}{\tau^3} \exp(x) \quad (22)$$

and *a=4.86, b=-13.08, c=12.76.* Therefore, the final equation can be written as

$$R(\mu,\mu_0,\varphi,\tau) = R_\infty^0 \exp\left(-y(1-0.05y)u(\mu,\mu_0,\varphi)\right) - (t-\Delta)e^{-x-y} K_0(\mu) K_0(\mu_0). \quad (23)$$

Eq. (23) is called the modified exponential approximation (MEA). We show the accuracy of MEA given by Eq. (23) in Figs. 2a,b for the nadir observation conditions, the solar zenith angle 60° and wavelengths 865nm and 2130nm. These wavelengths are often used in cloud retrieval techniques. Note that the single scattering albedo is equal to 1.0 and 0.9872 at these wavelengths, respectively. The asymmetry parameter is 0.8435 for the smaller wavelength. It is 0.8054 for the wavelength 2130nm. Exact data shown in Fig.2a are obtained using the vector radiative transfer code SCIAPOL (Rozanov and Kokhanovsky, 2006). The SCIAPOL is based on the discrete ordinate approach and thoroughly tested against tabular results presented by Siewert(2000). It follows that the accuracy of the approximation is better than 6% for the cloud optical thickness $\tau \geq 4$ in the case considered. Calculations performed for other angles show that the accuracy only weakly depends on the geometry providing that grazing observation and illumination conditions are excluded (Kokhanovsky and Rozanov, 2003). It means that the top-of-atmosphere reflectance over cloudy scenes can be accurately modeled in the framework of the MEA (even as compared to the vector radiative transfer model). One can see from Fig.2b that the accuracy of MEA could be increased if the exact result for the reflection function of a semi-infinite layer is used in calculations. Note that we used in Eq. (23) the following simple formula valid for the nadir observation conditions only (Kokhanovsky, 2002) :

$$R_{\infty}^{0}(\mu,\mu_0,\varphi)=\frac{0.37+1.94\mu_0}{1+\mu_0}. \qquad (24)$$

The results obtained with this equation are close to those derived from Eq. (12) at $\mu=1$. The accuracy of Eq. (24) can be further increased adding the function $F=0.25p(1-\arccos(\mu_0))$ to the nominator.

In addition, we show the accuracy of MEA as the function of the solar zenith angle in Figs. 3, 4. It follows that the accuracy is better than 5% for most of cases shown in Figs. 3, 4. Fig.3 underlines the physical principle behind the retrieval of τ. Fig. 4 shows that that the reflection function at the wavelength 1550nm is much more sensitive to the effective size of droplets as compared to the measurements of the reflectance at the wavelength 650nm (see Fig.3).

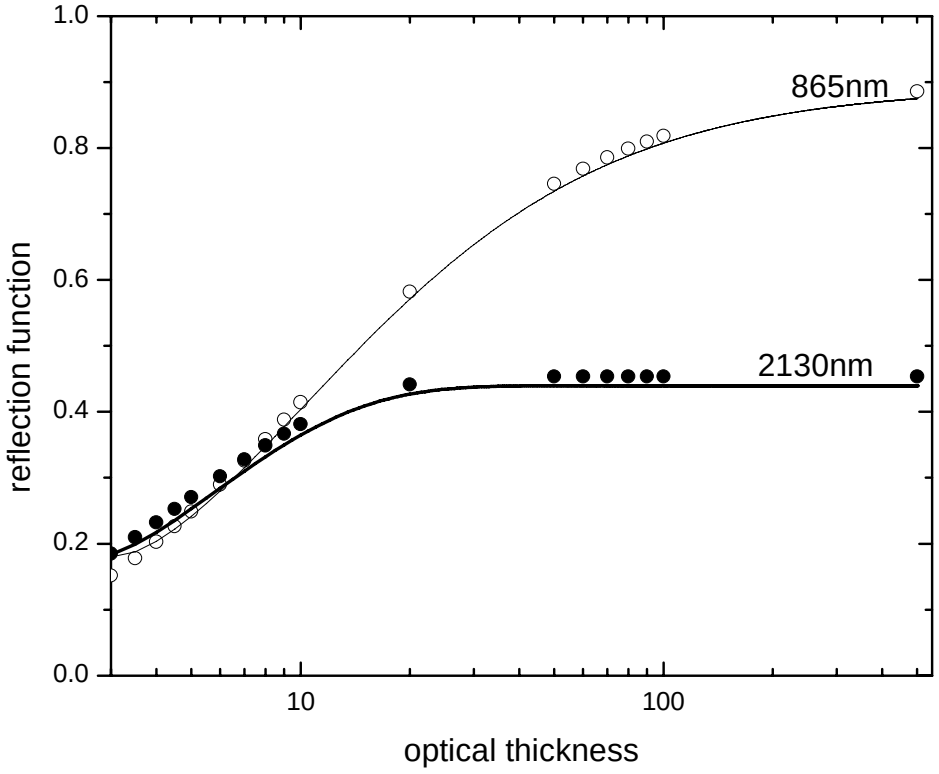

Fig.2a. Dependence of the reflection on the optical thickness for wavelengths 865nm and 2130nm at the nadir observation and the solar zenith angle 60 degrees. The effective radius of droplets is 6 μm and the coefficient of variance of the gamma particle size distribution is $1/\sqrt{7}$. Lines give the results according to MEA. Points show results of exact calculations using the vector radiative transfer code SCIAPOL. The following values of the refractive index *m* of water droplets have been used: *m=1.324*($\lambda=864nm$) and *m=1.29-0.0004i*($\lambda=2130nm$). The black underlying surface was assumed in the radiative transfer calculations.

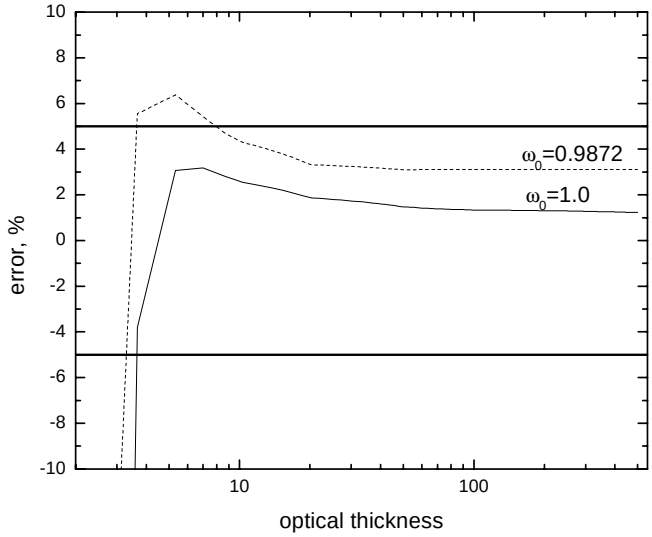

Fig.2b. The errors of MEA found from data given in Fig. 2a. The solid line with the higher value of the single scattering albedo corresponds to the wavelength 865nm. The broken line corresponds to results obtained for the wavelength 2130nm.

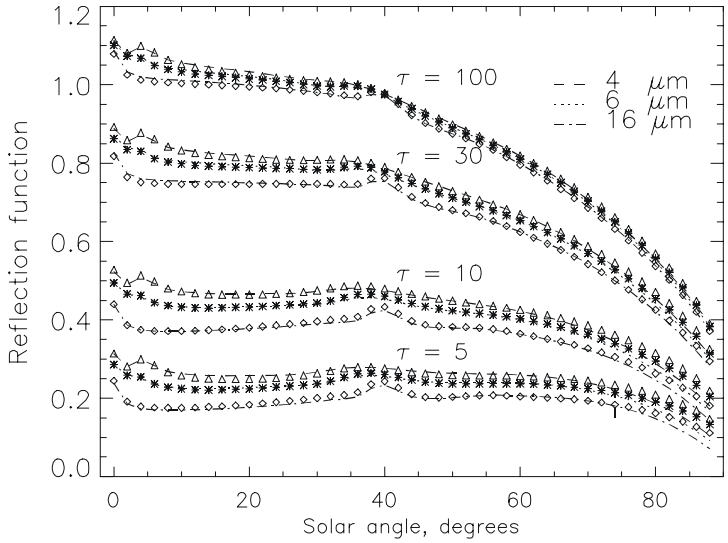

Fig. 3. Dependence of the reflection function on the solar angle for various values of the cloud optical thickness for the effective radius of droplets equal to 4, 6, and 16 at the wavelength 650nm and the nadir observation. The Deirmendjian Cloud C.1 (Deirmendjian, 1969) model of the droplet size distribution was assumed (with varied values of a_{ef}) . The black underlying surface is assumed. Symbols show exact radiative transfer calculations, lines correspond to the approximate analytical theory as described by Kokhanovsky and Rozanov (2003).

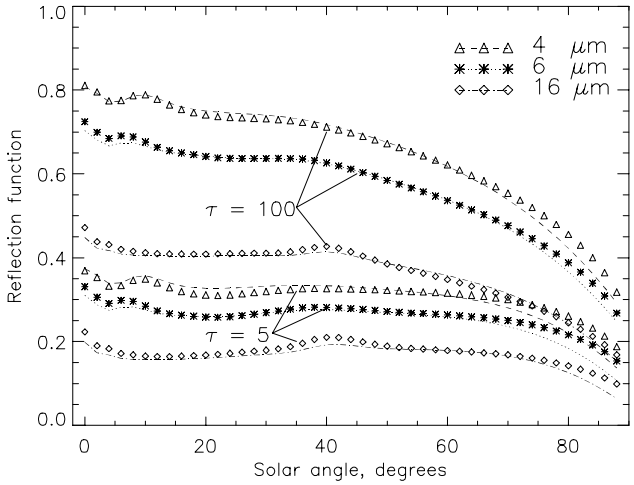

Fig. 4. Dependence of the reflection function on the solar angle for various sizes of droplets and the cloud optical thickness equal to 5 and 100 at the wavelength 1550 nm. The Deirmendjian Cloud C.1 (Deirmendjian, 1969) model of the droplet size distribution was assumed (with varied values of a_{ef}). The black underlying surface is assumed. Symbols show exact radiative transfer calculations, lines correspond to the approximate analytical theory as described by Kokhanovsky and Rozanov (2003).

2.4 Radiative transport in gaseous absorption bands

The exponential approximation presented above can be easily extended to account for the gaseous absorption. Then one should use the following substitutions in equations given above: $\tau \to \tau + \tau_g$, $\beta \to (\sigma_{abs} + \sigma_{abs,g}) / \left(\sigma_{ext} + \sigma_{abs,g}\right)$, where the subscript "g" relates the correspondent value to the gaseous absorption process. The phase function does not need to be modified because we ignore molecular scattering. This could be easily accounted for if necessary. However, we account for the additional light absorption in the atmosphere above a cloud. Therefore, it follows for the cloud reflection function $\bar{R}$ in the gaseous absorption band : $\bar{R} = T_1 R T_2$, where we omitted arguments for the simplicity. The value of *R* is given by Eq. (23) and $T_j = \exp(-m_j \tau_{abs})$, *j=1,2,* where $m_1 = 1/\mu_0$, $m_2 = 1/\mu$, and

$$\tau_{abs} = \sum_{i=1}^{N} \int_{z_1}^{z_2} C_{abs,i}(z)\varsigma_i(z)\,dz, \tag{25}$$

where $C_{abs,i}$ is the *i*th gas absorption cross section, *N* is the total number of gases present and $\varsigma_i(z)$ is the concentration of the *i*th gas at a given height. The integration extends from the upper cloud boundary position z_1 to the height of the optical instrument z_2. The accuracy of MEA for the gaseous absorption band can be increased if the single scattering contribution in the signal from the atmospheric layer above the cloud R_s is also taken into account. Then it follows:

$$\bar{R} = T_1 R T_2 + R_s \tag{26}$$

The expression for R_s is presented elsewhere (Kokhanovsky and Rozanov, 2004). We checked the accuracy of Eq. (26) with account for Eq. (23) performing exact calculations using the radiative transfer code SCIATRAN (Rozanov et al., 2005) for the oxygen absorption A-band located at the wavelengths 758-768nm. The atmospheric model used in calculations coincides with that described by Kokhanovsky and Rozanov (2004). The values of $\overline{R}$ are averaged with respect to the Gaussian instrument response function with the half-width 0.225nm. The absorption by the oxygen was accounted for by using the HITRAN 2000 (Rothman et al., 2003) database in conjunction with the correlated k-distribution approximation (Kokhanovsky and Rozanov, 2004). To increase the accuracy of the model, we accounted for light scattering and absorption below the cloud layer using the approximate technique developed by Kokhanovsky and Rozanov (2004). Results are given in Figs. 5-9. It follows from the analysis of the data presented that the accuracy of approximate calculations is better than 5% in most of cases. The errors increase for low clouds having larger values of τ due to the simplicity of our model, which accounts for the cloud – upper atmospheric layer interaction in a first coarse approximation only (Kokhanovsky and Rozanov, 2004). This interaction becomes more important for low thick clouds. Figs. 5, 9 illustrate the physical background behind the retrieval of the cloud top and bottom heights.

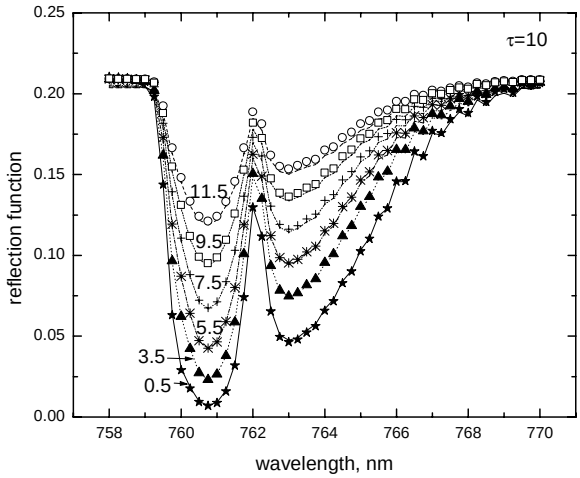

Fig.5. Dependence of the cloud reflection function on the wavelength in the oxygen A-band for cloud top heights equal to 0.5, 3.5, 5.5, 7.5, 9.5, 11.5 km at the cloud optical thickness $\tau = 10$. The cloud geometrical thickness is equal to 250m. The droplet size distribution and the illumination/viewing conditions coincide with that used in calculations presented in Fig.1. The atmospheric model used is identical to that described by Kokhanovsky and Rozanov(2004). Symbols give exact results obtained with SCIATRAN (Rozanov et al., 2005). Lines are plotted using Eq. (26).

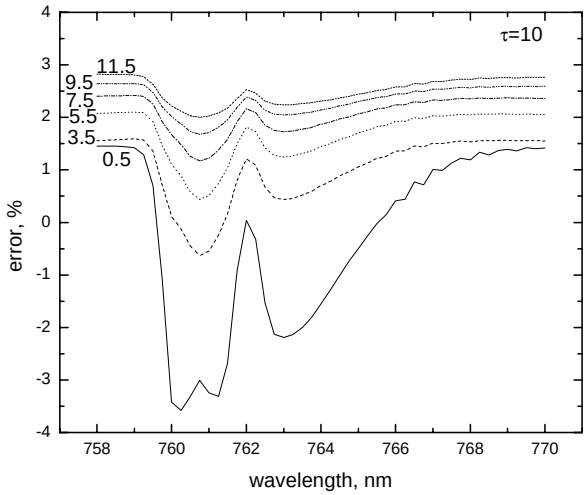

Fig. 6. The errors of Eq. (26) derived using data shown in Fig.5 for various cloud top height positions and $\tau = 10$.

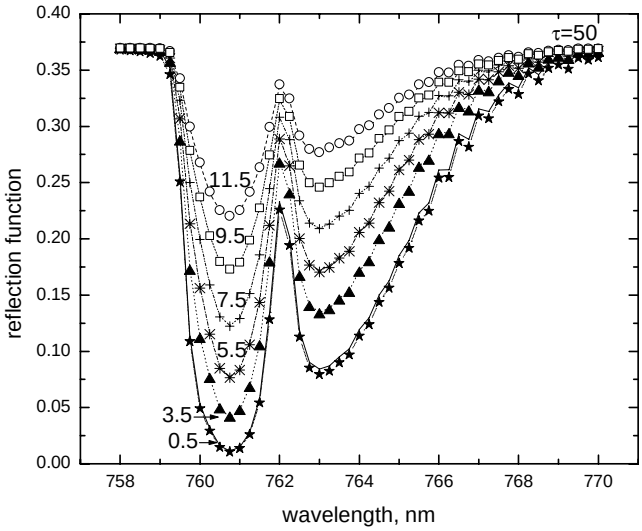

Fig.7. The same as in Fig.5 except at $\tau = 50$.

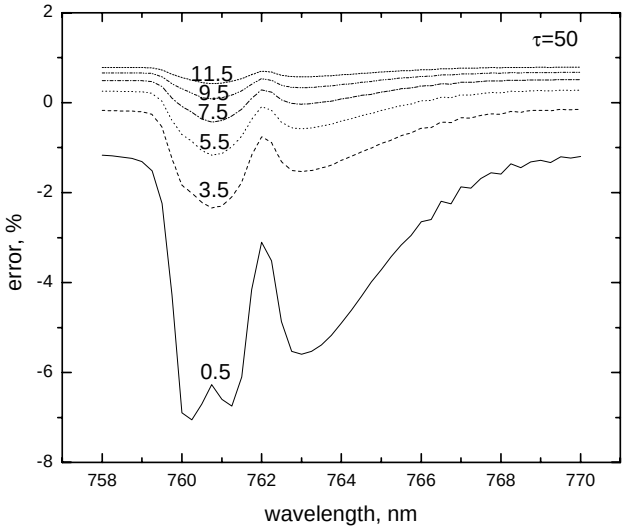

Fig. 8. The errors of Eq. (26) calculated using data shown in Fig.7 for various cloud top height positions and $\tau = 50$.

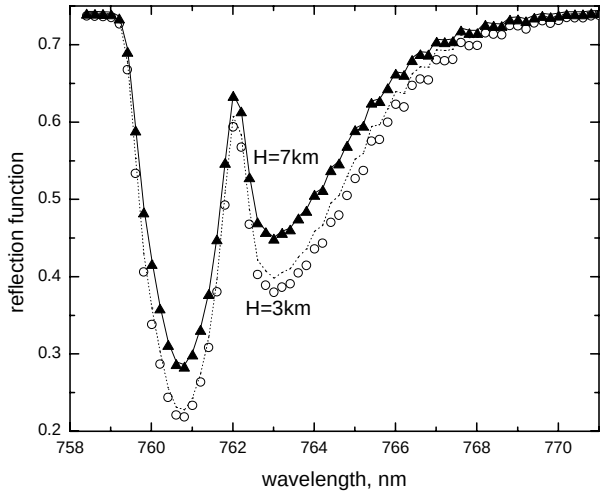

Fig. 9 Cloud reflection function in the oxygen A-band calculated using SCIATRAN (lines) (Rozanov et al., 2005) and asymptotic analytical theory (symbols) (Kokhanovsky and Rozanov, 2004) at the nadir observation, the solar zenith angle equal to 60 degrees, the optical thickness equal to 50, the cloud top height equal to 9km and cloud bottom height equal to 3km(circles) and 7km (circles). All other parameters needed to calculations (e.g., atmospheric vertical profiles) coincide with those described by Kokhanovsky and Rozanov (2004). The reflectance function is averaged with the step 0.2 nm using SCIAMACHY (Bovensmann et al., 1999) response function.

3. Inversion procedure

Equations given above are simple and can be applied for the development of a number of cloud retrieval algorithms for specific optical instruments. In this section we will describe the two uncoupled algorithms. One is for the determination of the cloud droplet radius and liquid water path (SACURA-A) and yet another one for the determination of the cloud optical thickness $\tau(758nm)$ and the cloud geometrical characteristics like cloud top height h and cloud geometrical thickness l (SACURA-B). Retrieved values of a_{ef} and w enable the determination of the spectral cloud optical thickness and also the cloud spherical albedo and the cloud droplet number concentration. One can use the retrieved pair (h ,l) to derive the cloud bottom height $h_b=h-l$.

The algorithms are the most accurate for completely cloud covered pixels. If cloud fraction is equal to c, then the reflection function of a cloudy part of the pixel R_c is found using the following linear relationship (see above):

$$R_c=c^{-1}R-c^{-1}(1-c)R_a, \tag{27}$$

where R_a is the reflectance of a clear atmosphere. The cloud fraction is obtained from Optical Cloud Recognition Algorithm (OCRA) (see below).

3.1. Liquid water path and effective radius

The SACURA is based on the two-wavelength semi-analytical cloud retrieval algorithm for the liquid water path (LWP) w and the cloud particle size (CPS) a_{ef} determination proposed by Kokhanovsky et al. (2003). The physical principle behind the retrieval could be easily understood analysing Figs. 3,4. It follows from these figures that the reflection function in the visible is primarily dependent on the cloud optical thickness (see Fig.3) (and, therefore, on the LWP) and the infrared channels are sensitive to the size of droplets (see Fig.4).

Parameters a_{ef} and w are used to find the cloud optical thickness $\tau(443nm)$ (Kokhanovsky et al., 2003):

$$\tau=\frac{1.5w}{\rho a_{ef}}\left\{1+\frac{1.1}{\left(ka_{ef}\right)^{2/3}}\right\}, \tag{28}$$

where $\rho=1\frac{g}{cm^3}$ is the density of water, $k=\frac{2\pi}{\lambda}$, λ is the wavelength. The cloud albedo r and the column droplet concentration N (not reported in the output) can be found from following approximate analytical equations valid in the visible (Kokhanovsky, 2004a):

$$r=\frac{1}{1.072+0.75\tau(1-g)}, \tag{29}$$

$$\mathrm{N}=\frac{\tau}{2\pi\varsigma a_{ef}^2}, \tag{30}$$

where $\varsigma=0.7$ and

$$g=0.88-\frac{1}{2ka_{ef}} \tag{31}$$

is the asymmetry parameter.

The values of a_{ef} and w are found from the system of two algebraic equations (Kokhanovsky et al., 2003):

$$R_1 = R_\infty^0 - \frac{t_1\left(a_{ef}, w\right)\left[1-A_1\right]}{1-A_1\left[1-t_1\left(a_{ef}, w\right)\right]} K_0\left(\vartheta\right) K_0\left(\vartheta_0\right) \tag{32}$$

$$\begin{aligned} R_2 &= R_\infty^0 \exp\left(-y_2\left(a_{ef}\right)\left(1-0.05 y_2\left(a_{ef}\right)\right)u \right) \\ &- \left[\exp\left(-x_2\left(a_{ef}, w\right) - y_2\left(a_{ef}\right)\right) - \frac{t_2\left(a_{ef}, w\right) A_2}{1-A_2 r_2\left(a_{ef}, w\right)} \right] t_2\left(a_{ef}, w\right) K_0\left(\vartheta\right) K_0\left(\vartheta_0\right). \end{aligned} \tag{33}$$

The subscripts " 1 " and " 2 " refer to wavelengths λ_1 and λ_2 in visible and near – infrared channels, respectively. R_1 and R_2 are measured reflection functions in the visible and infrared, respectively. Specifically, the SACURA uses measurements at the wavelengths 443nm and 1550nm. These channels are almost free of gaseous absorption. Values of A_1 and A_2 give us the surface albedos in the visible and near-infrared, respectively, ϑ_0 is the solar zenith angle, ϑ is the zenith observation angle. Other functions in Eqs. (32), (33) are given in Table 1.

Equations (32) and (33) have two unknowns (a_{ef} and w). Standard methods and programs are available for the solution of such problems. However, taking into account the specific form of Eq. (32), the exclusion method is used here. This allows a single transcendent equation with one unknown (a_{ef}) to be formulated. It follows from Eq. (32) that

$$t_1 = \left\{ \frac{K_0\left(\vartheta_0\right) K_0\left(\vartheta\right)}{R_{\infty 0} - R_1} - \frac{A_1}{1-A_1} \right\}^{-1} . \tag{34}$$

On the other hand, it follows from the formula for t_1 given in Table 1 in the visible:

$$\tau_1 = \frac{4\left(t_1^{-1} - 1.072\right)}{3\left(1-g_1\left(a_{ef}\right)\right)} . \tag{35}$$

The optical thickness τ_1 is related to the liquid water path w and the effective radius of droplets by the following equation (see Appendix 2):

$$\tau_1 = w\bar{\sigma}_{ext}\left(\lambda_1, a_{ef}\right) , \tag{36}$$

where

$$\bar{\sigma}_{ext} = \frac{1.5}{\rho a_{ef}}\left(1 + \frac{1.1}{\left(k a_{ef}\right)^{2/3}}\right) . \tag{37}$$

Therefore, the analytical expression for w can be obtained:

$$w = \frac{4\left(t_1^{-1} - 1.072\right)}{3\overline{\sigma}_{ext}\left(\lambda_1, a_{ef}\right)\left(1 - g_1(a_{ef})\right)}, \tag{38}$$

where the dependence of all functions on the value of the effective radius is explicitly shown. Thus, one unknown (w) is expressed in terms of another (a_{ef}). The substitution of Eq. (38) into Eq. (33) and the use of the formulae in Table 1 yields a single transcendent equation for the determination of the effective radius of droplets in a cloud. It should be pointed out that w enters Eq. (33) via $x_2\left(a_{ef}, w\right)$. The parameter y_2 in Eq. (33) does not depend on w by definition (see Table 1). The function $x_2\left(a_{ef}, w\right)$ can be written as :

$$x_2\left(a_{ef}, w\right) = \sqrt{3\left(1 - \omega_{02}\left(a_{ef}\right)\right)\left(1 - g_2\left(a_{ef}\right)\right)}\tau_2\left(a_{ef}, w\right), \tag{39}$$

where only τ_2 depends on the liquid water path w. The index "2" corresponds to the wavelength λ_2 in the near-infrared.

Taking into account the definition of the optical thickness: $\tau = \sigma_{ext} l$, where l is the cloud geometrical thickness and σ_{ext} is the extinction coefficient, τ_2 in Eq. (39) is given by : $\tau_2 = \Phi(a_{ef})\tau_1$. The analytical expression for the function

$$\Phi\left(a_{ef}\right) = \frac{\sigma_{ext}\left(\lambda_2\right)}{\sigma_{ext}\left(\lambda_1\right)} \tag{40}$$

is presented in Appendix 2 and τ_1 is given by Eq. (35). The value of t_1 is determined by Eq. (34).

Summing up, the substitution of the approximation shown above into Eq. (33) together with formulae for local optical characteristics of clouds, presented in Appendix 2, yields us a single equation for the effective radius retrieval from measurements of R_1 and R_2. This equation can be easily solved numerically. For this we have used the Brent's method of findinding roots (Brent, 1972; Press et al., 1992). The obtained value of a_{ef} is used to calculate the optical thickness at the wavelength 443nm, where the liquid water path is determined directly from Eq. (38). The value of the optical thickness is also reported at the wavelength 758nm. It is calculated from the reflectance at 758nm under assumption that the droplet effective radius is equal to 6 micrometers. Therefore, the reported value of the optical thickness at 443nm is more accurate one. It uses the information on a_{ef} retrieved as described above. The values r and N can be found using Eqs. (29), (30).

Table 1. Auxiliary functions. Further definitions are given in Appendix 2. The function $F(\theta)$ is calculated as $F(\theta)=\sum_{m=1}^{\infty} x_m\left[P_m(\cos\theta)-(-1)^m P_m(\cos\vartheta)P_m(\cos\vartheta_0)\right]$, where x_m are coefficients of the expansion of the phase function with respect to Legendre polynomials $P_m(\cos\theta)$ (Kokhanovsky, 2004b). Here θ is the scattering angle, ϑ_0 is the solar zenith angle, ϑ is the observation zenith angle, and φ is the relative azimuth.

The auxiliary function	Formula
u	$K_0(\vartheta)K_0(\vartheta_0)\left[R_\infty^0(\vartheta,\vartheta_0,\varphi)\right]^{-1}$
$K_0(\vartheta)$	$\frac{3}{7}(1+2\cos\vartheta)$
t_2	$t_c-\Delta$ $\Delta=(4.86\text{-}13.08\cos\vartheta_0\cos\vartheta+12.76\cos^2\vartheta_0\cos^2\vartheta)\exp(x_2)/\tau_2^3$
t_1	$\frac{1}{1.072+0.75\tau_1(1-g_1)}$
t_c	$\frac{\sinh y_2}{\sinh\left[x_2+1.07y_2\right]}$
r_2	$\exp(-y_2(1-0.05y_2))-t_c\exp(-x_2-y_2)$
x_j	$\gamma_j\tau_j$
y_j	$\frac{4\gamma_j}{3\left[1-g_j\right]}$
γ_j	$\sqrt{3(1-g_j)(1-\omega_{oj})}$
R_∞^0	$\frac{3.944-2.5(\cos\vartheta_0+\cos\vartheta)+10.664\cos\vartheta_0\cos\vartheta+F(\theta)}{4(\cos\vartheta+\cos\vartheta_0)}$

3.2 Cloud top height and cloud geometrical thickness

The determination of the cloud top height *h* using SACURA-B is based on the measurements of the top-of-atmosphere (TOA) reflection function *R* in the oxygen A-band (Kokhanovsky et al., 2004; Rozanov and Kokhanovsky, 2004; Rozanov et al., 2004). The spectral dependence $R(\lambda)$ of the cloud with the optical thickness 5 for the nadir observation and the solar angle equal to 60 degrees is shown in Fig. 5 for various cloud top heights. This Figure confirms that the cloud reflection function is extremely sensitive to the cloud top height in the center of the oxygen absorption band.

To find the value of *h*, we first assume that the TOA reflectance *R* can be presented in the form of a Taylor expansion around the assumed value of cloud top height equal to h_0:

$$R(h) = R(h_0) + \sum_{i=1}^{\infty} a_i (h - h_0)^i , \tag{41}$$

where $a_i = R^{(i)}(h_0)/i!$. Here $R^{(i)}(h_0)$ is the *i*-derivative of *R* at the point h_0. The next step is the linearization, which is a standard technique in the inversion procedures (Rozanov et al., 1998; Rozanov and Kokhanovsky, 2004; Rozanov et al., 2004; Rodgers, 2000). We found that the function *R(h)* is close to a linear one in a broad interval of the argument change (Kokhanovsky and Rozanov, 2004). Therefore, we neglect nonlinear terms in Eq. (41). Then it follows:

$$R = R(h_0) + R'(h_0)(h - h_0), \tag{42}$$

where $R' = \frac{dR}{dh}$. We assume that *R* is measured at several wavelengths in the oxygen A-band. Then instead of the scalar quantity *R* we can introduce the vector $\vec{R}_{mes}$ with components $\left(R(\lambda_1), R(\lambda_2), ...R(\lambda_n)\right)$. The same applies to other scalars in Eq. (41).

Therefore, Eq. (42) can be written in the following vector form:

$$\vec{y} = \vec{a}x \tag{43}$$

where $\vec{y} = \vec{R}_{mes} - \vec{R}(h_0)$, $\vec{a} = \vec{R}'(h_0)$, and $x = h - h_0$. Note that both measurement and model errors are contained in Eq. (43). The solution $\hat{x}$ of the inverse problem is obtained by minimizing the following cost function (Rodgers, 2000):

$$\Phi = \left\| \vec{y} - \vec{a}x \right\|^2 , \tag{44}$$

where $\| \ \|$ means the norm in the Euclid space of the correspondent dimension.

The value of $\hat{x}$, where the function Φ has a minimum can be presented as

$$\hat{x} = \frac{(\vec{y}, \vec{a})}{(\vec{a}, \vec{a})} = \frac{\sum_{i=1}^{n} a_i y_i}{\sum_{i=1}^{n} a_i^2} , \tag{45}$$

where $(,)$ denotes a scalar product in the Euclid space, *n* is the number of of spectral channels, where the reflection function is measured.

Therefore, from known values of the measured spectral reflection function R_{mes} (and also values of the calculated reflection function R and its derivative R' at $h = h_0$) at several wavelengths, the value of the cloud top height can be found from Eq. (45) and equality: $h = \hat{x} + h_0$. The value of h_0 is taken equal to 1.0 km, which is a typical value for low level clouds (Feigelson, 1982). The main assumption in our derivation is that the dependence of R on h can be presented by a linear function on the interval x (Kokhanovsky and Rozanov, 2004).

The SACURA-B code finds both the cloud top height h and the cloud geometrical thickness l simultaneously. This requires the minimization of the following cost function (see Eq. (44)):

$$\Phi = \left\| \vec{y} - \hat{A}\vec{X} \right\|^2 \tag{46}$$

The elements of the matrix $\hat{A}$ are correspondent weighting functions (Rodgers, 2000). The solution of the inverse problem is given by the vector-parameter $\vec{X}$. This vector has 5 components, which give corrections to the initially assumed cloud top height and cloud geometrical thickness, the correction to the initially assumed half-width of the spectrometer spectral response function, the shift parameter, and the squeeze parameter.

Clearly, first two parameters give us final values of the pair (h, l) to be retrieved. The third parameter allows to adjust the assumption on the instrument response function. Last two parameters allow to reduce errors related to the displacement of the experimentally measured spectrum due to the errors of the spectral calibration and the Doppler shift.

We have developed two versions of the retrieval algorithm. One is based on the exact radiative transfer calculations of the reflection function *R*. Yet another one is based on the approximate representation of R as described above(Kokhanovsky and Rozanov, 2004; Rozanov and Kokhanovsky, 2004; Rozanov et al., 2004).

We have used the correlated k-distribution method to account for the high-frequency oscillations of the oxygen molecule absorption cross section σ_a (Lacis and Oinas, 1991; Buchwitz, 2000; Buchwitz et al., 2000). The temperature and pressure dependence of σ_a for a given location of measurements was accounted for using the standard atmosphere model built in SCIATRAN (Rozanov et al, 2002). We have used the most recent version of the HITRAN molecular spectroscopic database to get data on cross sections σ_a (Rothman et al., 2003).

For the operational retrievals, we have used the retrieval technique based on the approximate representation of *R*. It allows us to speed up the retrieval process considerably.

4. Phase index and reflection function

SACURA also reports the phase index (PI)

$$\alpha = \frac{R(1550nm)}{R(1670nm)} \tag{47}$$

and reflectance R at 443nm. These parameters are obtained directly from measurements without application of any retrieval procedures. The value of α indicates the presence of ice clouds as indicated below. $R(443nm)$ is above 0.2 for cloud, snow, and ice. Therefore, this characteristic enables a quick estimation of the atmospheric or ground conditions during measurements. The wavelength 443 nm has been chosen because the surface reflectance contribution is weak for this wavelength both over land and ocean. Also this channel is used in other satellite spectrometers and radiometers (e.g., MERIS (Bezy et al., 2000)).

The thermodynamic state of a cloud is an important parameter for cloud physics and climate problems. It is known that spectral properties of ice differ significantly in the spectral range 1500-1700 nm from those of water (Pilewskie and Twomey, 1987; Knap et al., 2002). Therefore, we introduce the phase index (PI) α (see above) to characterize the thermodynamic state of a cloud. Low values of this parameter correspond to ice clouds.

We find using radiative transfer calculations that the value of α is in the range 0.8 - 1.0 for water clouds and it is in the range 0.5-0.7 for ice clouds (see Fig.10). Calculations were performed using the modified asymptotic equations given by Kokhanovsky and Rozanov (2003) in the assumptions that both crystals and droplets have the spherical shape. It was assumed that the cloud optical thickness is varied in the range 5-30 for both water and ice clouds. The effective radius of droplets in water clouds and also ice crystals was changed in the range 5-30 microns. Studies performed by Kokhanovsky et al. (2005) show that the increase of the size of particles increases the separation of both cloud types. Note that ice crystals have highly irregular shape and also the size is often in the range 100-500 microns. This will enhance differences even further. Calculations as shown in Fig.10 correspond to nadir observation and the solar angle of 60 degrees. We found that the change of the illumination angle does not influence the positions of regions with characteristics values of the PI for water/ice cloud significantly. Therefore, PI indeed can be used as an indicator of the cloud phase. More discussions on the phase index are given by Kokhanovsky et al. (2005).

Obviously, we have for clear sky over black surfaces: R(1550nm)>R(1670nm), and, therefore, $\alpha > 1$. Some highly reflecting soils could have values of $\alpha = 0.5 - 0.7$ similar to crystalline clouds. However, these pixels can be screened out using information on the derived cloud top pressure, the cloud optical thickness or both. There is no such a screening performed in the current version of SACURA.

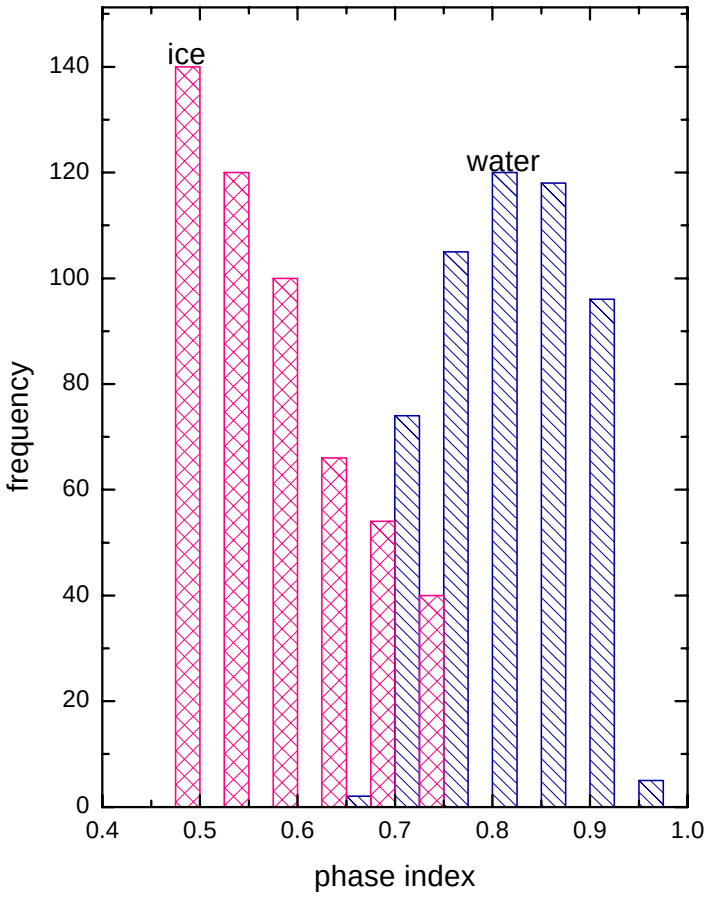

Fig.10. The cloud phase index (PI) frequency distribution (see details in the text).

5. Cloud fraction

The cloud fraction *c* is retrived using the Optical Cloud Recognition Algorithm(Loyola and Ruppert, 1998). OCRA separates measurements into two components: a cloud-free background and a remainder expressing the influence of clouds. The key to the algorithm is the construction of a cloud-free composite that is invariant with respect to the atmosphere, to topography and to solar and viewing angles for a given point of observation. Initial pre-processing is required before multi-temporal data can be fused to develop the composite. For a given location $M(x,y)$ (e.g., flat surface), the reflection function R is measured by the Polarization Measurement Devices (PMDs) of SCIAMACHY. Measurements at 310-365nm (PMD1, blue), 455-515nm (PMD2, green), and 610-690nm (PMD3, red) are used by OCRA. The measured reflectance is translated into normalized *rg*-color space via the relation:

$$r = \frac{R(x,y,\lambda_R)}{\sum_{i=R,G,B} R(x,y,\lambda_i)}, \quad g = \frac{R(x,y,\lambda_G)}{\sum_{i=R,G,B} R(x,y,\lambda_i)}, \tag{48}$$

where *B*, *G*, and *R* denote measurements obtained by PMD1, PMD2, and PMD3, respectively. We underline that PMDs have better spatial resolution than SCIAMACHY science pixels used in trace gas retrievals. This allows to detect the cloud structure of a large SCIAMACHY pixel (typically, 30*60km^2) using PMD measurements. Quantities *r* and *g* define a point in the *rg* chromaticity diagram (Loyola and Ruppert, 1998). By definition, the white point located at the position *W*(1/3, 1/3) in *r-g* space corresponds to a cloud. It is important to note that all clouds independently on their thickness are concentrated in the vicinity of the point *W*. The points correspondent to the minimal reflectance are located at positions A_j in *r-g* space. Measurements for partially cloudy positions for a given location *M*(*x*,*y*) are concentrated on the line WA$_j$ in the *rg* space. It means that it is possible to conceive the cloud fraction algorithm based on the location of a given measurement point on the length $L = [WA_j]$. A detailed description of the algorithm is given by Loyola (2000, 2004). By definition, the algorithm does not work over spectrally neutral surfaces (e.g., snow). Then it follows: $L \to 0$.

Tuinder et al.(2004) compared several algorithms for retrieving cloud fraction using GOME against synoptic surface observations made by human eye. The OCRA algorithm outperforms the other cloud fraction algorithms used in that comparison.

6. Calibration issues

We have used the SCIAMACHY Processor 5.01 data (June 1st, 2004). The following calibration coefficients ζ have been applied to the measured reflectances (Kokhanovsky et al., 2006): 1.07 for the wavelength λ_1=443nm and 1.15 for the wavelength λ_2=1550nm. So the retrievals were performed using not raw sun-normalized reflectances *R* but rather calibrated (by us) sun-normalized reflectances $\Re = \zeta R$. The details on the calibration of SCIAMACHY are given by Kokhanovsky et al. (2006).

To avoid oscillations as appear in experimental spectra, we make ratios shown in Eq. (47) not for the precise wavelengths as shown in Eq. (47) but for a small wavelength interval $(\Delta\lambda = 2nm)$ around the wavelengths given in Eq. (47).

7. Auxiliary data

The ground albedo and the ground height needed for the retrievals are taken from the SCIATRAN database (Rozanov et al., 2005) (see www.iup.physik.uni-bremen.de/sciatran). Correspondent databases are distributed freely together with SCIATRAN package. The ground albedo is taken equal to 0.294(sand), 0.195(soil), 0.908(snow), 0.410(vegetation), 0.012(water) depending on the pixel location. These numbers together with the latitude and longitude grid (and also ground top height grid) have been provided by R. Guzzi and T. Kurosu (personal communication). Profiles of temperature and pressure are taken from the MPI model (Bruhl and Crutzen, 1993). The

absorption cross section of oxygen is taken from HITRAN database (Rothman et al., 2003). The clear sky aerosol model is taken from Kneizys et al. (1996) at the visibility 23km. The further description of the clear atmosphere model used is given by Kokhanovsky and Rozanov (2004).

8. Validation

The validation of SACURA is ongoing activity far to be completed at this stage. Satellite derived products to be validated are:

- (1) cloud top height;
- (2) cloud bottom height;
- (3) cloud geometrical thickness;
- (4) cloud optical thickness;
- (5) droplet effective radius;
- (6) liquid water path;
- (7) cloud phase index.

Only the validation of cloud top height product has been performed up to date based on single radar (Kokhanovsky et al., 2004) measurements as far as application of SACURA to SCIAMACHY is of concern. These comparisons show up to $\pm$0.5-1.0km differences in the SACURA-retrieved cloud top heights on avearge. However, it must be remembered that lidars and radars provide measurements at single points whereas SCIAMACHY pixel size is 30*60km^2. SACURA as applied to GOME, which has a similar spectral but even worse spatial resolution, shows quite good correspondence as compared to ATSR-2 thermal infrared measurements (see Table 2). We expect to have a similar accuracy of SACURA as applied to SCIAMACHY data as compared to AATSR measurements. This is due to the similarities of these advanced optical instruments.

The comparison with AATSR retrievals is a matter of ongoing research. The correlation plot of GOME-SACURA-derived CTHs as compared to IR ATSR-2 measurements is shown in Fig.12. The SACURA-derived CTH are on average by 0.5 km higher as compared to collocated IR measurements (see Table 2 and Figs.12, 13). Fig. 14 confirms that biases are larger for thicker clouds. This may indicate the problem with multi-layered cloudiness. All retrievals using SACURA are performed in the assumption of a homogeneous single cloud layer composed of water droplets.

Table 2. Average CTHs as retrieved using data from ATSR-2 $\left(\left\langle H_{IR}\right\rangle\right)$ and GOME $\left(\left\langle H_{s}\right\rangle\right)$. Statistical data results given in km. Brackets signify average values. It follows: $\left\langle B_{s}\right\rangle=\left\langle H_{s}\right\rangle-\left\langle H_{IR}\right\rangle$. The standard deviation is denoted by σ. The geographical position of orbits studied is given in Fig. 11.

Orbit	15453 04.04.1998	16910 15.07.1998	18366 25.10.1998	19537 14.01.1999	All orbits
Number of pixels	234	159	325	214	931
$< H_{IR} >$	6.5	6.6	5.9	6.4	6.4 ± 0.3
$< H_{s} >$	6.5	6.8	7.0	7.2	6.9 ± 0.3
$< B_{s} >$	-0.1	0.1	1.1	0.8	0.6 ± 0.6
σ_{s}	1.6	1.5	2.1	2.2	1.8 ± 0.4

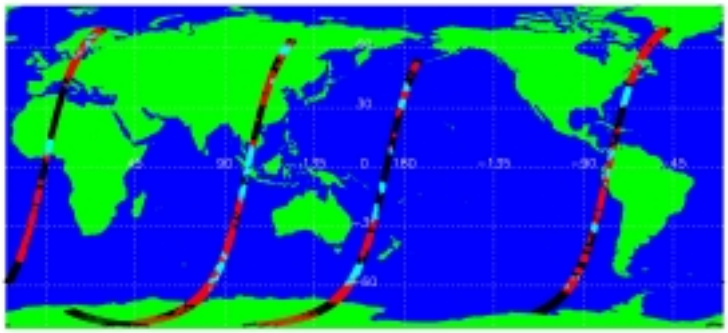

Fig.11. Position of selected ERS-2 orbits 16910, 18366, 19537, and 15453. Numbers are counted from left to right (the orbit 16910 is over Europe and Africa). Areas with cloud top heights below 7km are marked in red and those with cloud top heights above 7km are marked in blue. Black areas correspond to cloud free scenes.

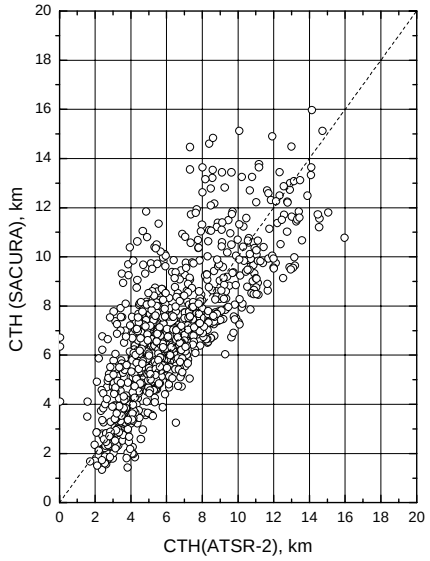

Fig.12. Correlation plot between CTHs obtained using SACURA and thermal IR measurements of ATSR-2.

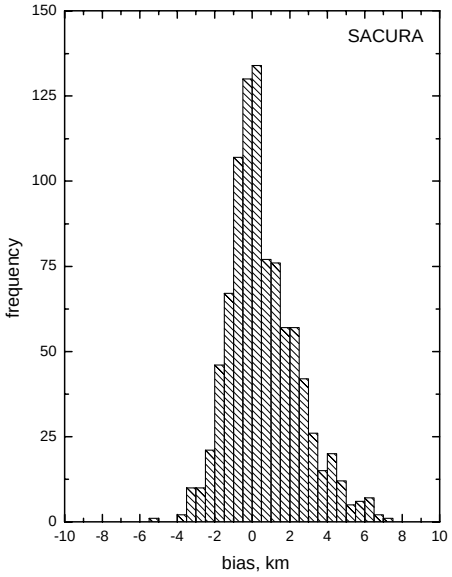

Fig.13. Histogram of biases of SACURA GOME - derived CTHs as compared to those derived using thermal IR measurements of ATSR-2.

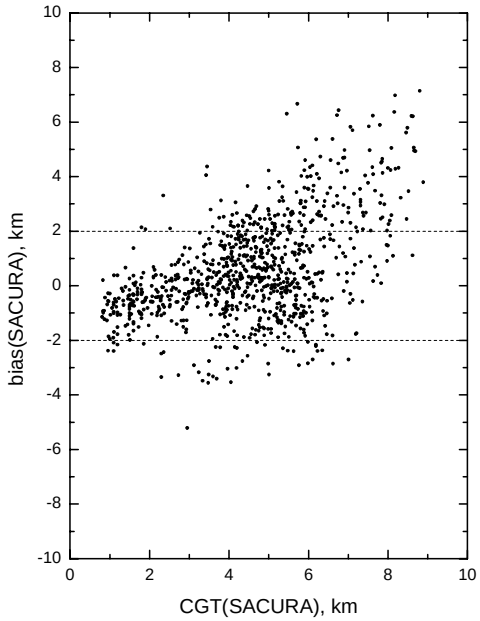

Fig.14. Dependence of the SACURA bias B_s on the cloud geometrical thickness.

9. Recommendations for the validation.

The cloud optical thickness and cloud effective radius can be validated using collocated AATSR or MODIS measurements. The cloud bottom height product can be validated using the ground radar measurements (e.g., KNMI radar). Such activities are planned for future research. Currently, the comparison of the cloud top heights retrieved by SACURA using SCIMACHY data with airborne lidar measurements is undertaken.

10. Sensitivity and error analysis

Although both aerosol (Kokhanovsky, 2001) and molecular (Bucholtz, 1995) scattering and absorption are neglected, their influence is minimized by a careful selection of spectral channels. Also, the influence of molecular and aerosol scattering is of importance mostly for $\tau < 5$ (Wang and King, 1997). This range of optical thicknesses is out of scope of the applicability of the algorithm described.

The applicability of the algorithm proposed for the optical thickness retrieval is limited both from the side of small $(\tau < 5)$ and large $(\tau \geq 100)$ values of the optical thickness (Kokhanovsky et al., 2003). However, the appearance of such clouds in the Earth's atmosphere is rare as indicated by Trishchenko et al.(2001). For the effective radius retrieval, however, there is no upper boundary for large τ. This is due to the fact that the reflection of light depends on the size of droplets even for an infinitely thick absorbing cloud. The same applied to the cloud top height.

The comprehensive error analysis of SACURA products has been performed by Kokhanovsky et al. (2003) and Rozanov and Kokhanovsky (2004). The comparison of

SACURA with other cloud remote sensing algorithms was performed by Nauss et al. (2005).

We consider now the sensitivity and error analysis for each product now. The results are obtained generated measured spectra with SCIATRAN, then introducing an error in these spectra and checking how algorithm responds to these errors.

Results for a_{ef} and τ are given in Figs. 4, 5. It follows from the analysis of these figures that the error of measurement of about 10% results in almost the same error in the cloud optical thickness and at least 1.5 times larger error in a_{ef} for the cases considered in Figs. 4, 5. These estimations are valid for 100% cloud covered pixels only. The error in τ and a_{ef} is strongly influenced by the correct information with respect to cloud fraction. In particular, it is expected that a_{ef} retrieved over broken cloud fields will be overestimated due to unknown contribution from the ground.

Typical simulated cloud top height errors are given in Fig. 17. It follows that errors are in the range 50-200m and they are negative. Therefore, SACURA on average overestimates CTH.

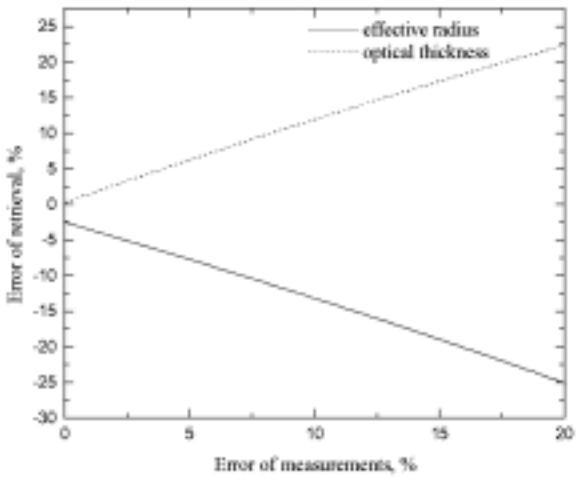

Fig. 15. The error of retrieval of the effective radius and cloud optical thickness as the function of the error of measurements. The synthetic spectra were calculated at the solar zenith angle 49 degrees, the observation angle 7 degrees, and the relative azimuth zero degrees. It was assumed that the effective radius of droplets is equal to 10 micrometers and cloud optical thickness is equal to 10 (Kokhanovsky et al., 2003).

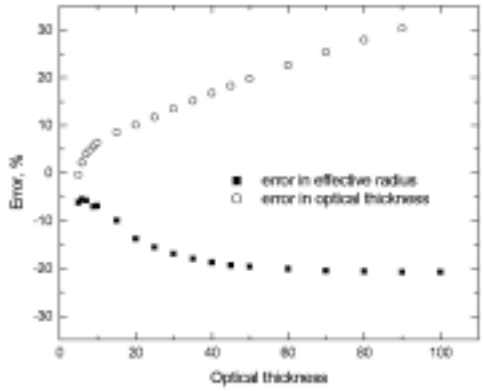

Fig.16. The same as in Fig. 15 except as the function of the cloud optical thickness.

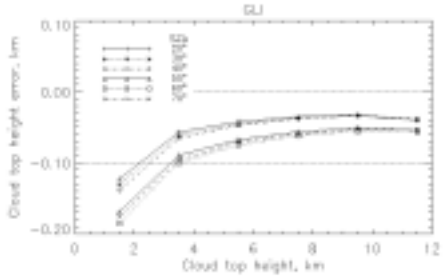

Fig. 17. The simulated SACURA error as the function of the cloud top height for various solar zenith angles. Negative values of the error mean too large retrieved values of the cloud top height. The simulations have been performed at the cloud geometrical thickness equal to 0.5km and the cloud optical thickness equal to 30 for the nadir observation conditions (Rozanov and Kokhanovsky, 2006).

SACURA is the dynamic software package, which is under development at the moment. In particular, it has following shortcomings:

- There is no a special retrieval chain for ice clouds.
- The vertical and horizontal inhomogeneity of clouds is not accounted for.
- The cloud top structure (e.g., shadows) is not accounted for.
- The possible existence of multi-layered cloudiness is not accounted for.
- The calibration of raw SCIAMACHY data should be refined.
- The results are valid for optically thick clouds only($\tau > 5$).

- The surface model is too simplified and must be improved considerably. This issue, however, is of less importance for completely cloudy pixels.
- The influence of the clear sky model on the retrieval has not been studied. Such a study is planned in future.
- The ground height model must be updated to the last available data. This is only of importance for retrievals over land surfaces.

11. Conclusions

A system of analytical equations has been developed , which can be used to retrieve the effective radius of droplets and the liquid water path of optically thick clouds ($\tau \geq 5$). Also we find other cloud characteristics such as:

- the optical thickness;
- the phase index;
- the cloud top height.

We give maps of the optical thickness, the effective radius, the liquid water path, the phase index, R(443nm), the cloud fraction as derived from OCRA using GOME surface reflectance database as a single .pdf file at our website for a particular orbit. These files are accompanied by the numerical data.

The cloud top height is determined using spectral measurements in the 758-770 nm oxygen A-band and the phase index is determined using differences in the refractive index of liquid water as compared to ice in the spectral range 1550-1670nm. Such spectral measurements are routinely performed by the SCIAMACHY instrument (Bovensmann et al., 1999).

One important feature of the algorithms proposed is its simplicity. It can be included as an integrated and autonomous part of operational cloud satellite retrieval schemes. It is characterized by a high accuracy and has important advantages as compared to the standard fitting methods used in up-to-date cloud retrieval schemes (especially if the speed of calculations is a concern as it is often the case in the analysis of large data bases).

Acknowledgements

Authors are grateful to A. Piters for important comments and help. They also thank D. Loyola for help with respect to cloud fraction algorithm implemented in the SACURA retrieval chain and to T. Nauss for the work related to the intercomparison of SACURA retrievals with products obtained by other cloud retrieval algorithms.

Appendix 1. Auxiliary functions and parameters.

The simulated reflection function needed for finding the cloud top height h is presented as follows: $\bar{R} = R_s + T_1 R T_2$, where it follows(Kokhanovsky and Rozanov, 2004):

$$R_s = \frac{1}{4\xi\eta}\int_h^H dz\left(\sigma_{sca}^R(z)\,p^R(\theta) + \sigma_{sca}^A(z)\,p^A(\theta,z)\right)\exp\left[-\tau(z)\left(\mu_0^{-1}+\mu^{-1}\right)\right], \quad \text{(A1.1)}$$

$$\mathrm{T} \equiv T_1 T_2 = \exp\left[-\tau'\left(\mu_0^{-1} + \mu^{-1}\right)\right] \tag{A1.2}$$

and

$$\tau' = \sum_{i=1}^{M} \int_h^H C^G{}_{abs,i}(z) c_i(z)\, dz. \tag{A1.3}$$

Here $C^G_{abs,i}(z)$ is the *i-th* gas absorption cross section, M is the total number of gases present, c_i is the *i-th* gas concentration, ξ and η are cosines of incidence and observation angles, respectively. H is the top of atmosphere height, assumed to be equal to 60 km. Only extinction due to light absorption by gases is present in τ'.

Parameters in Eq. (A1.1) have the following meaning (see also Kokhanovsky and Rozanov (2004)):

- $\sigma^A_{sca}(z)$ and $\sigma^R_{sca}(z)$ are total aerosol and Rayleigh scattering coefficients, respectively;
- $p^A(\theta, z)$ and $p^R(\theta)$ are aerosol and Rayleigh phase functions, respectively;
- $\tau(z)$ is the optical depth of the atmosphere above z along the vertical axis OZ, which includes the contribution from both molecular and aerosol scattering and absorption.

The value of R is calculated using Eq. (23), where y_2 is determined by the single scattering albedo ω_0. The single scattering albedo ω_0 is defined by the following equation:

$$\omega_0 = 1 - \frac{\sigma_{abs}}{\sigma_{ext}}, \tag{A1.4}$$

where

$$\sigma_{abs} = \sigma^A{}_{abs} + \sigma^G{}_{abs} + \sigma^C{}_{abs}, \tag{A1.5}$$

$$\sigma_{ext} = \sigma^A{}_{ext} + \sigma^G{}_{ext} + \sigma^C{}_{ext}, \tag{A1.6}$$

where indices *A*, *G* and *C* show aerosol, gas, and cloud contributions, respectively, to extinction σ_{ext} and absorption σ_{abs} coefficients.

Let us assume that $\sigma^A{}_{abs} = \sigma^C_{abs} = 0$. Then we have

$$\omega_0 = 1 - \frac{\sigma^G{}_{abs}}{\sigma_{ext}}. \tag{A1.7}$$

Thus, the value of ω_0 changes with the height both inside and outside of a cloud. Eq. (23) for the cloud reflection, however, is applicable only for the case of a vertically homogeneous layer. The dependence $\omega_0(z)$ is not particularly strong in the area, where a cloud is present. Therefore, we adopt here the model of an "effective homogeneous layer" (Yanovitskij, 1997). In this case one should find the height inside the cloud at which the value of ω_0 should be taken for calculations. Details of this are given by Kokhanovsky and Rozanov (2004). Note that we also have accounted for the variation of the cloud liquid water content with the height *z* (the adiabatic profile).

Appendix 2. Integral light scattering and absorption characteristics.

Integral light scattering and absorption characteristics of a water cloud can be found with following equations (Kokhanovsky, 2001, 2006):

$$\sigma_{ext} = \sigma^*_{ext} C_v \qquad (A.2.1)$$

$$\sigma_{abs} = \sigma^*_{abs} C_v, \qquad (A.2.2)$$

$$1 - g = 0.12 + 0.5\left(ka_{ef}\right)^{-2/3} - 0.15\kappa a_{ef}\,, \qquad (A.2.3)$$

where

$$C_v = \mathrm{N}\langle V \rangle \qquad (A.2.4)$$

is the volumetric concentration of droplets, N is the number of droplets in a unit volume of a cloud, $\langle V \rangle$ is the average volume of a droplet in a unit volume of a cloudy medium, $k = 2\pi/\lambda$, λ is the wavelength, a_{ef} is the effective radius of droplets, $\kappa = 4\pi\chi/\lambda$, χ is the imaginary part of the refractive index of water, g is the asymmetry parameter, σ_{ext} and σ_{abs} are extinction and absorption coefficients . The values of σ^*_{ext} and σ^*_{abs} are given by (Kokhanovsky, 2001, 2006):

$$\sigma^*_{ext} = \frac{1.5}{a_{ef}}\left(1 + \frac{1.1}{\left(ka_{ef}\right)^{2/3}}\right), \qquad (A.2.5)$$

$$\sigma^*_{abs} = \frac{5\pi\chi\left(1-\kappa a_{ef}\right)}{\lambda}\left(1 + 0.34\left(1 - \exp\left(-\frac{8\lambda}{a_{ef}}\right)\right)\right). \qquad (A.2.6)$$

It follows from Eqs. (A. 2.1) , (A.2.5) for the ratio of extinction coefficients (and also for the ratio of optical thicknesses) at two wavelengths:

$$\Phi = \left(\frac{\lambda_2}{\lambda_1}\right)^{2/3} \frac{1.1 + \varsigma_2^{2/3}}{1.1 + \varsigma_1^{2/3}}\,, \qquad (A.2.7)$$

where, $\varsigma_j = \dfrac{2\pi a_{ef}}{\lambda_j}$, $j=1,2$. Note that we have for large values of $\varsigma_j \to \infty$: $\Phi \to 1$. The optical thickness is given by:

$$\tau = \sigma_{ext} l\,, \qquad (A.2.8)$$

where L is the geometrical thickness of a cloud. It follows from Eqs. (A. 2.1), (A. 2. 7):

$$\tau = \bar{\sigma}_{ext} w, \qquad (A.2.9)$$

where $w = \rho C_v L$ is the liquid water path, ρ is the density of water, $\bar{\sigma}_{ext} = \sigma^*_{ext} / \rho$. The accuracy of Eqs. (A.2.3) - (A.2.6) has been studied as compared to exact Mie calculations by Kokhanovsky and Zege (1995, 1997) and Kokhanovsky (2001). The error is smaller than 5 - 8% at $\lambda < 2.2 \mu m$.

If higher accuracy is needed one can use the direct parameterization of the Mie calculations. We obtain with the accuracy better than 1% at selected wavelengths free of gaseous absorption:

$$1 - g = \sum_{n=0}^{4} c_n \left(k a_{ef} \right)^{-2n/3} , \qquad \sigma_{abs} = \frac{4\pi\chi}{\lambda} C_v \sum_{n=0}^{4} d_n \left(k a_{ef} \right)^n , \qquad (A.2.10)$$

where constants c_n, d_n are presented in Tables A. 1, A. 2 at $\lambda = 0.6457$, 0.8590, 1.239 and 1.549 micrometers. There is no need to modify Eq. (A.2.5) due to its high accuracy.

At larger wavelengths it is easier to make parametrizations of parameters y and $z = x / w$ (see Table 1) than σ_{ext}, σ_{abs}, 1 - g. In particular, it follows at $\lambda = 2.3 \mu m$:

$$y = 0.24206 + 0.02524 k a_{ef} - 1.4197 \cdot 10^{-4} k^2 a_{ef}^2 , \qquad (A.2.11)$$

$$z = 0.02008 - 0.54709 k a_{ef}^{-2/3} + 7.53062 (k a_{ef})^{-4/3} - 15.152 (k a_{ef})^{-2} . \qquad (A.2.12)$$

Note, that the value of y is dimensionless. The dimension of z coincides with that of w.

SACURA uses measurements at wavelengths 443nm and 1550nm. The refractive index for liquid water is assumed to be equal to 1.34 at 443nm and 1.31-0.000135i at 1550nm (Segelstein, 1981).

Table A. 1. Parameters c_i for different wavelengths λ .

$\lambda, \mu m$	c_0	c_1	c_2	c_3	c_4
0.6457	0.1121	0.5118	0.8997	0.0	0.0
0.8590	0.1115	0.4513	1.2719	0.0	0.0
1.239	0.1095	0.4198	1.5796	0.0	0.0
1.549	0.0608	2.465	-32.98	248.94	-636

Table A. 2 Parameters d_i for different wavelengths λ ($d_4 = 0$ at $\lambda = 1.239 \mu m$ and $d_4 = -0.00000001$ at $\lambda = 1.550 \mu m$).

$\lambda, \mu m$	d_0	d_1	d_2	d_3
1.239	1.779	-0.0068	0.0000494	-0.00000014
1.549	1.671	0.0025	-0.0002365	0.00000286

References

Acarreta J. R. et al. (2004): First retrieval of cloud phase from SCIAMACHY spectra around 1.6 μ m, *Atmos. Res.*, 72, 89-105.

Arking, A., and J.D. Childs (1985): Retrieval of clouds cover parameters from multispectral satellite images, *J. Appl. Meteorol., 24*, 323-333.

Bezy, J. L., S. Delwart, and M. Rast, 2000: MERIS- a new generation of ocean-colour sensor onboard ENVISAT, *ESA Bulletin*, 103, 48-56.

Bovensmann H. et al.(1999): SCIAMACHY: Mission objectives and measurement modes, *J. Atmos. Sci*., 56, 127-150.

Brent, R. P. (1973): *Algorithms for the Minimization Without Derivatives*, Englewood Cliffs: Printice Hall.

Bruhl, Ch., and P. J. Crutzen, 1993: MPIC Two-dimensional model, in : The atmospheric effects of stratospheric aircraft, NASA Ref. Publ.,1292,103-104.

Bucholtz, A. (1995): Rayleigh-scattering calculations for the terrestrial atmosphere, *Appl. Opt., 34*, 2765-2773.

Buchwitz, M. (2000): Strahlungstransport- und Inversions- Algorithmen zur Ableitung Atmospharischer Spurengasinformationen aus Erdfernerkundungsmessungen in Nadirgeometrie im ultravioletten bis nahinfraroten Spektralbereich am Beispiel SCIAMACHY, *PhD thesis,* Bremen: Bremen University.

Buchwitz, M., V. V. Rozanov, and J. P. Burrows (2000): A correlated-k distribution scheme for overlapping gases suitable for retrieval of atmospheric constituents from moderate resolution radiance measurements in the visible/near-infrared spectral region, *J. Geophys. Res., D105*, 15247-15262.

Cahalan, R.F., et al. (1994): The albedo of fractal stratocumulus clouds, *J. Atmos. Sci., 51*, 2434-2455.

Deirmendjian, A. (1969): *Electromagnetic Scattering on Spherical Polydispersions*, Amsterdam: Elsevier.

Deschamps, P.-Y. et al. (1994):The POLDER Mission: Instrument characteristics and scientific objectives, *IEEE Trans., GE 32*, 598-614.

Feigelson, E. M., ed. (1981): *Radiation in a Cloudy Atmosphere*. Leningrad: Gidrometeoizdat, 280 pp.

Fischer, J., et al. (2000): Cloud top pressure, MERIS Algorithm Theoretical Basis Document No ATBD 2.3, Berlin: Free University of Berlin.
Goloub, P. et al.(2000): Cloud thermodynamical phase classification from the POLDER spaceborne instrument, *J. Geophys. Res.:D, 105*, 14747-14759.

Germogenova, T. A. (1961): On the properties of the transport equation for a plane-parallel layer, *J. Appl. Math. Comp. Phys.*, 1, 928-946.

Germogenova, T. A.(1963): Some formulas to solve the transfer equation in the plane layer problem, in *Spectroscopy of Scattering Media, (AN BSSR, Minsk, 1963) ed. by B. I. Stepanov , 36-41*.

Han Q. et al.(1994): Near global survey of effective droplet radii in liquid water clouds using ISCCP data, *J. Climate, 7*, 465-497.

King, M.D. (1981): A method for determining the single scattering albedo of clouds through observation of the internal scattered radiation field, *J. Atmos. Sci., 38*, 2031-2044.

King, M.D. (1987): Determination of the scaled optical thickness of clouds from reflected soar radiation measurements, *J. Atmos. Sci., 44*, 1734-1751.

King, M.D., et al(1992):Remote sensing of cloud, aerosol, and water vapour properties from the moderate resolution imaging spectrometer (MODIS), *IEEE Trans., GE, 30*, 2-27.

Knap, W. H., P. Stammes, and R. B. A. Koelemeijer (2002): Cloud thermodynamic phase determination from near-infrared spectra of reflected sunlight, *J. Atmos. Sci., 59*, 83-96.

Kneizys, F. X. , et al.,1996: The MODTRAN 2/3 report on LOWTRAN-7 model (ed. by L. W. Abreu and G. P. Anderson), contract F19628-91-C-0132 with Ontar Corp., 261 pp., Philips Lab., Geophys. Dir., Hancom AFB, Mass.

Koelemeijer, R. B. A., P. Stammes, J. W. Hovenier, and J. F. De Haan (2001): A fast method for retrieval of cloud parameters using oxygen A band measurements from GOME, *J. Geophys. Res.*, 106, 3475-3490.

Koelemeijer, R. B. A., P. Stammes, J. W. Hovenier, and J. F. De Haan (2002): Global distributions of effective cloud fraction and cloud top pressure derived from oxygen A band spectra measured by the Global Ozone Monitoring Experiment: comparison to ISCCP data, *J. Geophys. Res.*, 107, 10.1029/2001JD000840.

Kokhanovsky, A.A., and E.P. Zege (1995): Local optical parameters of spherical polydispersions: simple approximations, *Appl. Opt., 34*, 5513-5519.

Kokhanovsky, A. A., and E. P. Zege (1997): Physical parametrization of local optical characteristics of cloudy media. *Izvestiya RAN, Fizika Atmosfer i Okeana*, 33, 209-218.
Kokhanovsky, A. A. (2001) *Light Scattering Media Optics*, Berlin: Springer-Praxis.

Kokhanovsky, A. A. (2002): Simple approximate formula for the reflection function of a homogeneous, semi-infinite turbid medium, *J. Opt. Soc. America,* A19, 957-960.

Kokhanovsky, A. A. et al. (2003) A semianalytical cloud retrieval algorithm using backscattered radiation in 0.4-2.4 μm spectral region, *J. Geophys. Res.*, D108, 4008, doi: 10.1029/2001JD001543.

Kokhanovsky, A. A., and V. V. Rozanov (2003): The reflection function of optically thick weakly absorbing layers: a simple approximation, *J. Quant. Spectr. and Rad. Transfer*, 2003, 77, 165-175.

Kokhanovsky, A. A. (2004a): Optical properties of terrestrial clouds, *Earth-Sci. Rev.*, 64, 189-241.

Kokhanovsky, A. A. (2004b): Reflection of light from nonabsorbing semi-infinite cloudy media: a simple approximation, *J. Quant. Spectr. Rad. Transfer,* 85, 25-33.

Kokhanovsky, A. A. (2006): *Cloud Optics*, Dordrecht: Springer-Verlag.

Kokhanovsky, A. A., and V. V. Rozanov (2004): The physical parameterization of the top-of-atmosphere reflection function for a cloudy atmosphere – underlying surface system: the oxygen A-band case study, *J. Quant. Spectr. and Rad. Transfer,* 85, 35-55.

Kokhanovsky, A. A., et al. (2004): The determination of a cloud altitude using SCIAMACHY on board ENVISAT, *IEEE Trans. Geosc. and Rem. Sens., Letters,* 1, 211-214.

Kokhanovsky, A. A., et al. (2005): The SCIAMACHY cloud products: algorithms and examples from ENVISAT, Adv. Space Res., 36, 789-799.

Kokhanovsky, A. A., et al. (2006): The semianalytical cloud retrieval algorithm for SCIAMACHY. II. The application to MERIS and SCIAMACHY data, *Atmos. Chem. Phys. Discussions,* in press.

Kondratyev K. Ya., and V.I. Binenko (1984): *Impact of Cloudiness on Radiation and Climate*, Leningrad: Gidrometeoizdat.

Kuji, M., and T. Nakajima (2002): Retrieval of cloud geometrical parameters using remote sensing data, Utah: CD-Proc. of 11th Conference on Atmospheric Radiation, JP1.7.

Kuze, A., and K. V. Chance (1994): Analysis of cloud top height and cloud coverage from satellites using the O_2 A and B bands, *J. Geophys. Res.*, 99, 14481-14491.

Lacis, A. A., and V. Oinas (1991): A description of the correlated k distribution method for modeling nongray gaseous absorption, thermal emission, and multiple scattering in vertically inhomogeneous atmospheres, *J. Geophys. Res., D96*, 9027-9063.

Liou, K. N. (1992): *Radiation and Cloud Processes in the Atmosphere,* Oxford: Oxford Univ. Press.

Loeb, N. G., and R. Davies (1996): Observational evidence of plane parallel model biases: Apparent dependence of cloud optical depth on solar zenith angle, *J. Geophys. Res., 101*, 1621-1634.

Loeb, N. G., and J. A. Coakley, Jr. (1998): Inference of marine stratus cloud optical depths from satellite measurements: Does 1D theory apply?, *J. Atmos. Sci., 11*, 215-233.

Loyola, D., and T. Ruppert, 1998: A new PMD cloud-recognition algorithm for GOME, *ESA Earth Observation Quarterly*, *58*, 45-47.

Loyola, D., 2000: Cloud retrieval for SCIAMACHY, *ERS-ENVISAT Symposium*, Gothenburg.

Loyola, D., 2004: Automatic cloud analysis from polar-orbiting satellites using neural network and data fusion techniques, *IEEE International Geoscience and Remote Sensing Symposium,* 4, 2530-2534.

Minin, I. N., 1988: *Radiative Transfer Theory*, Moscow: Nauka.

Mishchenko M.I., J.M. Dlugach, E.G. Yanovitskij, and N.T. Zakharova (1999): Bidirectional reflectance of flat, optically thick particulate layers: An efficient radiative transfer solution and applications to snow and soil surfaces. *J. Quant. Spectrosc. Radiat. Transfer* 63, 409-432.

Nakajima T. and M. D. King (1990): Determination of the optical thickness and effective particle radius of clouds from reflected solar radiation measurements. Part I. Theory, *J. Atmos. Sci.,* **47**, 1878-1893.

Nakajima, T. and M. D. King (1991): Determination of the optical thickness and effective particle radius of clouds from reflected solar radiation measurements. Part II. Marine stratocumulus observations, *J. Atmos. Sci.,* **48**, 728-750.

Nakajima, T. Y. et al. (1998): Optimization of the Advanced Earth Observing Satellite II Global Imager channels by use of the raduiative transfer calculations, *Appl. Opt.,* **37**, 3149-3163.

Naus, T., et al. (2005): The intercomparison of selected cloud retrieval algorithms, *Atmos. Res.*, 78, 46-78.

Pilewskie, P., and S. Twomey (1987): Discrimination of ice from water in clouds by optical remote sensing, *Atmos. Res*., 21, 113-122.

Platnick S. et al. (2001): A solar reflectance method for retrieving the optical thickness and droplet size of liquid water clouds over snow and ice surfaces, *J. Geophys. Res.,* **106**, D14, 15,185-15,199.

Press, W. H., et al. (1992): *Numerical Receipes in FORTRAN. The Art of Scientific Computing*, 2nd Edition, Cambridge: Cambridge University Press.

Rodgers, C. (2000): *Inverse Methods for Atmospheric Sounding: Theory and Practice*, Singapore: World Scientific.

Rossow, W. B. (1989): Measuring cloud properties from space: A review, *J. Climate, 2*, 419-458.

Rossow, W. B. and R. A. Schiffer (1999): Advances in understanding clouds from ISCCP, *Bul. Amer. Meteor. Soc.,* **80,** 2261-2287.

Rothman, L. S., et al. (2003): The HITRAN molecular spectroscopic database: edition of 2000 including updates through 2001, *J. Quant. Spectr. Radiat. Transfer,* 82, 5-44.

Rozanov, A. V., et al. (2005): SCIATRAN 2.0- A new radiative transfer model for geophysical applications in the 175-2400nm spectral region, *Adv. Space Res.*, 36, 1015-1019.

Rozanov, V. V., T. Kurosu, J. P. Burrows (1998): Retrieval of atmospheric constituents in the UV-Visible: a new quasi-analytical approach for the calculation of weighting functions, *J. Quant. Spectr. Radiat. Transfer, 60*, 277-299.

Rozanov, V.V. , M. Buchwitz, K.-U., Eichmann, R. de Beek, J. P. Burrows (2002): SCIATRAN – a new radiative transfer model for geophysical applications in the 240-2400 nm spectral range: The pseudo-spherical version, *Adv. Space Res*., *29*, 1831-1835.

Rozanov, V. V., A. A. Kokhanovsky (2004): Semi-analytical cloud retrieval algorithm as applied to the cloud top altitude and the cloud geometrical thickness determination from top of atmosphere reflectance measurements in the oxygen absorption bands, *JGR, 109*, D05202, doi: 10.1029/2003JD004104.

Rozanov, V. V., A. A. Kokhanovsky, J. P. Burrows (2004): The determination of cloud altitudes using GOME reflectance spectra: multilayered cloud systems, *IEEE Trans. Geosci. Rem. Sens.*, 42, 1009-1017.

Rozanov, V. V., A. A. Kokhanovsky (2006): The solution of the vector radiative transfer equation using the discrete ordinate technique: se;lected applications, *Atmos. Res.*, 79, 3-4, 241-265.

Rozenberg ,G. V. et al.(1978): The determination of optical characteristics of clouds from measurements of the reflected solar radiation using data from the Sputnik "KOSMOS-320", *Izvestiya Acad. Sci. USSR, Fizika Atmos. Okeana,* **10,** *14-24.*

Segelstein D. J. (1981): The complex refractive index of water, University of Missouri-Kansas City.

Slingo, A. (1989): A GCM parameterization for the shortwave radiative properties of water clouds, *J. Atmos. Sci., 46*, 1419-1427.

Trishchenko, A. P. et al. (2001): Cloud optical depth and TOA fluxes: comparison between satellite and surface retrievals from multiple platforms, *Gephys. Res. Let.*, **28**, 979-982.

Tuinder O. N. E., R. de Winter-Sorkina, and P. J. H. Builtjes, 2004: Retrieval methods of effective cloud cover for the GOME instrument: an intercomparison, *Atmos. Chem. Phys.*, Vol. 4, pp 255-273.

Van de Hulst, H. C. (1980): *Multiple Light Scattering: Tables, Formulas and Applications*, Academic Press.
Wang, M., and M. D. King (1997): Correction of Rayleigh scattering effects in cloud optical thickness retrievals, *J. Geophys. Res.*, **102**, D22, 25, 915-25,926.

Yamomoto, G., and D. Q. Wark (1961) Discussion of letter by A. Hanel: Determination of cloud altitude from a satellite, *J. Geophys. Res.*, 66, 3596.

Yanovitskij, E.G.(1997): *Light Scattering in Inhomogeneous Atmospheres*, N.Y.: Springer-Verlag.

Zege, E.P., A.P.Ivanov, and I.L. Katsev (1991): *Image Transfer Through a Scattering Medium*, New York: Springer-Verlag.